ACADEMIC PRESS

Available online at www.sciencedirect.com
SCIENCE DIRECT®

NeuroImage

NeuroImage 20 (2003) 479–488

www.elsevier.com/locate/ynimg

Differences in the hemodynamic response to event-related motor and visual paradigms as measured by near-infrared spectroscopy

G. Jasdzewski,[a,*] G. Strangman,[a,b] J. Wagner,[a] K.K. Kwong,[a] R.A. Poldrack,[a] and D.A. Boas[a]

[a] *Athinoula M. Martinos Center, Massachusetts General Hospital, Harvard Medical School, 149 13th St., Charlestown, MA 02129, USA*
[b] *Neural Systems Group, Massachusetts General Hospital, Harvard Medical School and Harvard-MIT Division of Health Sciences and Technology, Charlestown, MA, USA*

Received 6 May 2002; revised 24 January 2003; accepted 27 May 2003

Abstract

Several current brain imaging techniques rest on the assumption of a tight coupling between neural activity and hemodynamic response. The nature of this neurovascular coupling, however, is not completely understood. There is some evidence for a decoupling of these processes at the onset of neural activity, which manifests itself as a momentary increase in the relative concentration of deoxyhemoglobin (HbR). The existence of this early component of the hemodynamic response function, however, is controversial, as it is inconsistently found. Near infrared spectroscopy (NIRS) allows quantification of levels of oxyhemoglobin (HbO_2) and HbR during task performance in humans. We acquired NIRS data during performance of simple motor and visual tasks, using rapid-presentation event-related paradigms. Our results demonstrate that rapid, event-related NIRS can provide robust estimates of the hemodynamic response without artifacts due to low-frequency signal components, unlike data from blocked designs. In both the motor and visual data the onset of the increase in HbO_2 occurs before HbR decreases, and there is a poststimulus undershoot. Our results also show that total blood volume (HbT) drops before HbO_2 and undershoots baseline, raising a new issue for neurovascular models. We did not find early deoxygenation in the motor data using physiologically plausible values for the differential pathlength factor, but did find one in the visual data. We suggest that this difference, which is consistent with functional magnetic resonance imaging (fMRI) data, may be attributable to different capillary transit times in these cortices.

Introduction

Near infrared spectroscopy (NIRS) is a noninvasive optical recording technique that can measure brain activity in vivo by detecting features of the hemodynamic response of the brain to neural activity. It has several advantages over PET and fMRI, which also measure hemodynamic response parameters, in that it combines reasonable spatial resolution with a temporal resolution of ~1–10 ms. This excellent temporal resolution makes it possible to filter out noisy signals associated with physiological processes (e.g., Gratton and Corballis, 1995). Additionally, the ability to gather spectroscopic information with NIRS allows one to separately characterize changes in oxyhemoglobin and deoxyhemoglobin—an ability that affords a less ambiguous analysis of activity-induced volume and metabolic changes than (e.g.) blood oxygen level-dependent (BOLD) fMRI alone. Optical techniques such as NIRS are therefore well suited to study the nature of neurovascular coupling. NIRS has the added virtues of being portable and relatively low cost, allowing for its routine use with subjects of all ages (including infants) and in situations where PET and fMRI scans are unaffordable or impossible (e.g., in settings requiring substantial motion, even at bedside).

NIRS has been used to study a variety of neuronal processes, including vision (e.g., Villringer et al., 1993; Meek et al., 1995; Wobst et al., 2001), the motor and/or somatosensory system (e.g., Beese et al., 1998; Obrig et al.,

* Corresponding author. Building 149, 13th Street, Charlestown, MA 02129. Fax: +1-617-726-7422.
E-mail address: gary@nmr.mgh.harvard.edu (G. Jasdzewski).

1053-8119/03/$ – see front matter © 2003 Elsevier Inc. All rights reserved.
doi:10.1016/S1053-8119(03)00311-2

1996b; Steinbrink et al., 2000), as well as higher cognitive functions such as language (e.g., Hock et al., 1997; Sakatani et al., 1998; Watanabe et al., 1998), and frontal brain activation with the Wisconsin Card Sorting Task (Fallgatter and Strik, 1998). These studies have generally relied on blocked designs where stimuli are presented for a period lasting from a few seconds to several minutes, followed by a period of rest or fixation. In contrast to blocked designs are event-related designs, which have been used by EEG researchers for decades and more recently with fMRI (Buckner et al., 1996). It has been shown that single event designs can be successfully used with NIRS (Obrig et al., 2000), but since the peak response in a region is considerably smaller with an event-related design than with a blocked design, it is an open question whether rapid presentation event-related designs, which assume that hemodynamic responses are linearly additive (Boynton et al., 1996), can be successfully used with current NIRS instruments. A recently published study (Schroeter et al., 2002) indicates that such designs can be used to study cognitive processes with NIRS when the interstimulus interval is as long as 12 sec. We extend this further by collecting event-related data with an interstimulus interval as small as 5 s.

An important benefit of event-related experimental designs for NIRS is that they more efficiently average and reduce the contribution of confounding physiological signals. Previous research by our lab (Boas et al., 2002) and elsewhere (Wobst et al., 2001) indicates that data generated from stimuli presented in a blocked manner can include signals generated from physiological processes such as breathing and heart rate, and Mayer waves (low-frequency arterial pressure fluctuations), all of which are possibly physiological responses synchronized with the stimulus (Franceschini et al., 2000). The influence of these physiological processes on the detected signals is a matter of particular concern for experimental tasks eliciting changes in the measured hemodynamic parameters with amplitudes similar in magnitude to those elicited by the background physiological processes themselves (Gratton and Corballis, 1995).

An important attribute of the NIRS technique is its ability to separate out the oxyhemoglobin and deoxyhemoglobin contributions to the hemodynamic response function, making it suitable for exploring issues related to the hemodynamic response function. Issues that we examine here include the onset times of HbO, HbT, and HbR, early deoxygenation, the time to peak response of these species, and the poststimulus response.

The early deoxygenation occurs during the first several seconds of the hemodynamic response at the locus of neural activity after the presentation of a brief stimulus, which is then followed by a more pronounced decrease in deoxygenation as oxyhemoglobin flows into the area (Frostig et al., 1990). This so-called “initial dip” may be important for improving spatial localization of the neuronal signal. Evidence for early deoxygenation comes from fMRI and invasive optical imaging. It has been reported in research involving several species including the cat (Frostig et al., 1990), the rat (Jones et al., 2001), and the human (Menon et al., 1995; Hu et al., 1997); yet the very existence of the dip is a matter of controversy, for it is inconsistently found. Because those who find the dip have generally studied the visual cortex and those who do not find the dip have not, we tested the hypothesis that different parts of the cortex behave differently with respect to their hemodynamic response functions. In this study, we compared the hemodynamic response functions generated from human motor and visual cortices using rapid presentation event-related paradigms, finding significant differences between the areas. We also examine the poststimulus recovery of the response function and find that the poststimulus overshoot of the deoxyhemoglobin cannot be described by the common explanation of a delayed recovery of the total hemoglobin concentration (Mandeville et al., 1998; Leite et al., 2002). We discuss these results in the context of vascular models.

Materials and methods

Instrumentation

The MGH-NIRS system consists of two source lasers and four detectors. The sources were low-power laser diodes emitting light at discrete wavelengths, 682 and 830 nm (Hitachi, HL8325G). A stabilized current, intensity modulated by an approximately 5-kHz square wave at a 50% duty cycle, powered both lasers. The lasers were driven at the same frequency, but phase-shifted by 90° with respect to one another. This phase encoding—known as an in-phase/quadrature-phase (IQ) circuit—allows simultaneous laser operation as well as a method for isolating the wavelength information at each detector via lock-in detection.

The light from each source was directly coupled using standard SMA connectors fed into a 9 foot long bifurcated glass fiber bundle with a nominal 1.0 mm core diameter (Fiberoptics Technology, prototype). This source fiber guides the light to the scalp of the subject. Detector fibers are also glass fiber bundles, typically with a larger core diameter (2.7 mm) but still capable of fitting inside an SMA connector.

The four separate detector modules (Hamamatsu C5460-01) are optically and electrically isolated from each other. Each module consists of a silicon avalanche photodiode (APD) with a built-in high-speed current-to-voltage amplifier, and temperature-compensation. They achieve a gain of typically 10^8 V/W with a noise equivalent power of 0.04 p W/$(\text{Hz})^{1/2}$ resulting from the high detector sensitivity. Each detector output signal can be amplified individually via the custom acquisition software (described below). The incoming signal at a given detector is composed of both source colors, which are separated by synchronous (lock-in) detection using the two source signals as a reference. The output

of the decoding portion of the IQ circuit includes two signal components, corresponding to the two laser wavelengths. These two components are hereafter referred to as channels.

The signals of all eight channels (two colors for each of four detectors) were low-pass filtered with an analog cutoff frequency at 3 Hz for investigations of the slow vascular response. The custom data acquisition software enables the user to choose input range and sample rate of the ADC card of up to 16 kHz, as well as to optimize the gain for each detector. We used a sample rate of 200 Hz. Recorded data are stored as an ASCII file and analyzed with Matlab (Mathworks Inc.).

Motor paradigm

Subjects

Thirteen healthy subjects were examined (9 female, 4 male; mean age of 27.1 years). Each subject consented to the experimental procedure, which was approved by the Massachusetts General Hospital internal review board. Subjects laid on their backs on a comfortable pad in a dark and quiet room, with their heads turned slightly to their right so as to be able to see a laptop Macintosh screen. The experiment consisted of 3 event-related runs. Each run was 10 min in length and consisted of 60 trials, with a mean ISI of 8 s. Each trial was 2 s in duration, and trials were spaced between 2 and 33 s apart. Previous research has shown that it is possible to deconvolve trials spaced as close as 2 s (Dale and Buckner, 1997). The precise timing of the events was selected by software that produces a sequence of event starting times to optimize the convolution (Dale et al., 1999). Subjects fixated on a laptop screen that presented the words "STOP" and "GO" alternately. When they saw GO, they opened and closed their right hands at a rate of approximately 3 Hz for 2 s. They stopped moving when the screen presented the word STOP.

Optode localization

The optical fiber bundles (optodes) were attached to a flexible piece of plastic that was in turn attached to a Velcro headband that was fastened snugly around the head of the subject. Each detector was 3.3 cm from the source, which was placed roughly between points C3 and Cz in the 10–20 system. One detector was then placed over the top of the head, roughly corresponding to point Cz in the 10–20 system (see Fig. 1). Since the optodes were all attached to the piece of plastic, their relative positions did not change from subject to subject. It can be reasonably assumed that with this positioning of the optodes that the primary sensorimotor cortex is part of the sampling volume (Homan et al., 1987; Steinmetz et al., 1989).

Visual paradigm

Subjects

Five healthy subjects were examined (4 female; mean age of 24.75 years). Each subject consented to the experimental procedure, which was approved by the Massachusetts General Hospital internal review board. Subjects sat upright in a comfortable chair in a dark and quiet room, so as to be able to see a laptop Macintosh screen, upon which flashed (2 Hz) a counterphasing checkerboard. The experiment consisted of 4 runs. Each run was 7 1/2 min long and consisted of 90 trials, 2 s in duration. Mean ISI was 5 s with intervals ranging from 2 to 21 seconds.

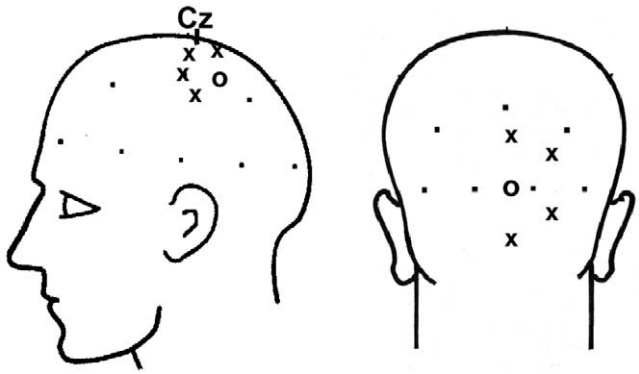

Fig. 1. Optode placement for motor (on left) and visual (on right) paradigms. "0" marks the location of the sources, while "X" marks the location of the detectors.

Optode localization

Optodes were attached as in the motor task, again with each detector 3.3 cm from the source. The center of the probe was placed approximately 1 cm to the right of the subject's inion (see Fig. 1). From such a placement, source-detector pairs should be sensitive to primary and secondary visual cortex (Homan et al., 1987; Steinmetz et al., 1989).

Data analysis

Subjects were excluded from averaging if their raw data failed to show a plausible heart rate ($n = 4$ for motor, 1 for visual) or exhibited large motion artifacts ($n = 1$ for motor). For the motor data, 8 of the original subjects were retained for further analysis, using 3 runs of 60 trials each for a grand total of 1440 trials. For the visual data, 4 of the original 5 subjects were retained for further analysis, using 4 runs of 90 trials each for a grand total of 1440 trials as well.

The raw 200-Hz data were offset-corrected, digitally low-pass filtered at 1 Hz, down sampled to 2 Hz, converted to OD units, and then high-pass filtered with a cutoff frequency of 1/30 Hz to remove any slowly drifting signal components. Finally, each signal pair was converted to relative changes in the concentration of HbR and HbO_2 for each channel using the modified Beer-Lambert Law, the principle of which is described in detail elsewhere (Cope and Delpy, 1988; Chance, 1991; Villringer and Chance, 1997). This equation requires an assumption regarding the differential path lengths traveled by the two laser-light colors. No existing assumptions (Kohl et al., 1998; Obrig et al.,

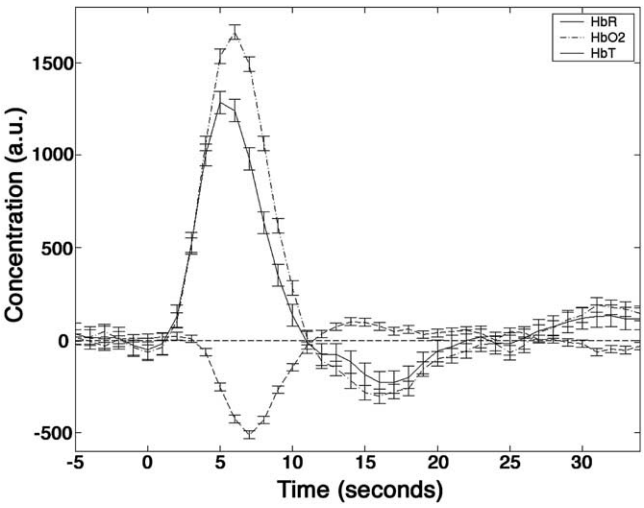

Fig. 2. Motor data of (HbR, HbO2, and HbT) analyzed with differential pathlength factors of 6 and 6 for 682 and 830 nm, respectively. Error bars indicate the standard errors.

2000) are without problems, suggesting a need for further theoretical work (Boas et al., 2001). In the absence of such work and given the similar total absorption magnitudes for 682 and 830 nm light in tissue, we chose our differential pathlength factor (DPF) to be the same for both wavelengths of a given source-detector combination and equal to 6 (Duncan et al., 1995). We then compared the results of this with those obtained when we analyzed the data using 6 for the 830 laser and several different values for the 682 laser (3–12 in increments of 0.5). We did not vary the DPF for the one laser for convenience, as it is the ratio between DPF values that is significant in the analysis. This variation allowed us to examine the effect of pathlength factor systematic errors on the interpretation of the hemoglobin signals. This is particularly important given that the early increase in deoxyhemoglobin (the "dip") can result from an incorrect choice of pathlength factors, and that the dip has been shown to disappear in some cases when using different pathlength factors (Mayhew et al., 1999; Kohl et al., 2000; Boas et al., 2001; Lindauer et al., 2001).

Statistical analysis was performed for individual subjects using the general linear model as outlined by (Burock and Dale, 2000) and implemented using the FS-FAST analysis package (Burock and Dale, 2000). Functionally, the analysis requires a deconvolution of the (randomly occurring) stimulus onset times from each recorded time series and averaging the resulting hemodynamic responses across subjects. Specifically, the stimulus paradigm was modeled using a set of delta functions at regular (0.5 s) intervals of peristimulus time (from -5 to $+$ 35 s), such that the resulting amplitude estimates reflect the estimated event-related response at each point in peri-stimulus time. The covariance of noise was not estimated (i.e., white noise was assumed). The approach makes no assumptions about the nature of the hemodynamic response other than the fact that multiple overlapping responses will add linearly. After estimation of amplitudes and variances at each time point, statistical parametric maps were created across all source-detector pairs for both HbR and HbO2 using linear contrasts of parameter estimates. In order to achieve unbiased detection of responses with any time course, maps were computed using the maximally significant response across the entire time course (Bonferroni corrected). Statistically maps were thresholded $P = 0.05$ (uncorrected). From these results, one source-detector pair was chosen for further analysis across subjects using a *t* test based on fixed-effect averaging.

Results

Fig. 2 shows the average time courses for the changes in [HbR], [HbO2], and total hemoglobin [HbT] from all 1440 trials (or events) of the motor task. The curves were generated using a constant differential pathlength factors analysis (i.e., 6 and 6 for both wavelengths). Fig. 3 shows the same information for the visual task.

In both data sets the typical hemodynamic response pattern is evident, with a task-related increase in HbO_2 concentration and a decrease in the relative concentration of HbR. The response is delayed by approximately 2 s. In the motor data (Fig. 2) the onset of the rise in HbO_2 precedes that of the decrease in HbR, and HbO_2 peaks at ~6 s while HbR peaks at ~7 s and HbT peaks at ~5 s. There is a poststimulus overshoot of HbR peaking around 14 s that slowly returns to baseline.

The visual data (Fig. 3) is qualitatively similar to the motor data but there are also notable differences. A striking difference is that HbR is first observed to increase along with an HbO_2 decrease at 1–2 s followed by an HbO_2 and HbT increase at 3 s and an HbR decrease at 4 s. And unlike the motor data, the peak time for HbO_2, HbR, and HbT is

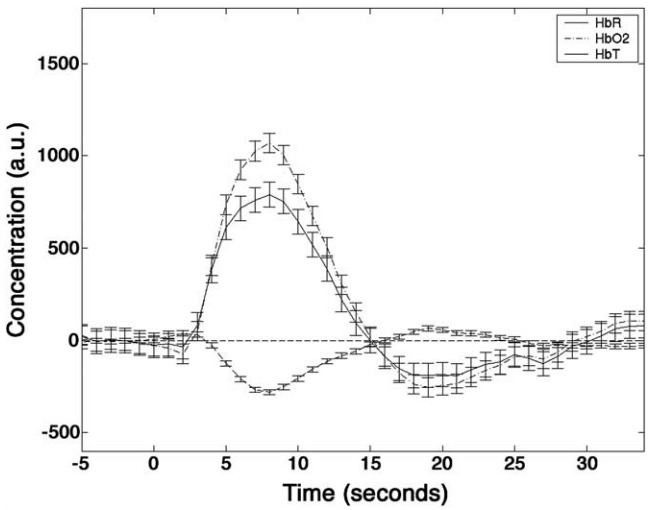

Fig. 3. Visual data of (HbR, HbO_2, and HbT) analyzed with differential pathlength factors of 6 and 6 for 682 and 830 nm, respectively.

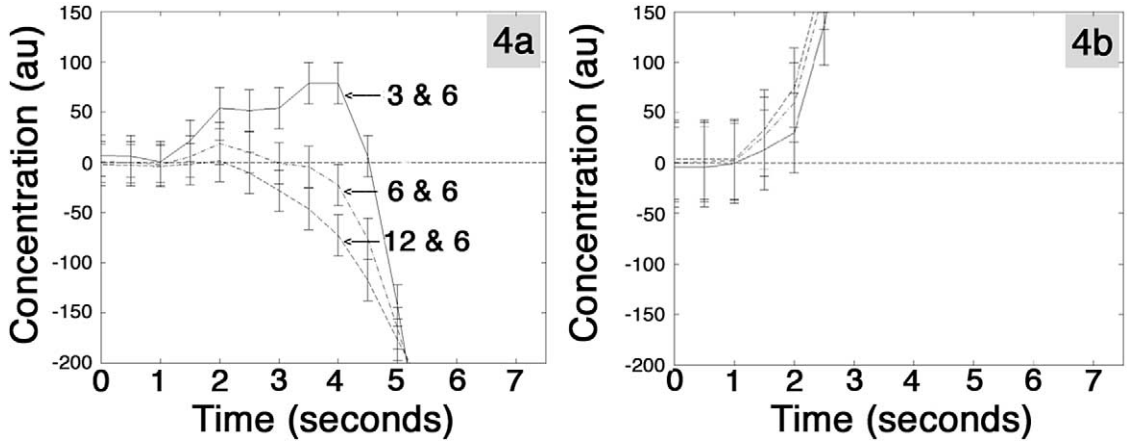

Fig. 4. Initial (a) HbR and (b) HbO_2 response to the motor task analyzed with 3 different differential pathlength factor pairs: 3 and 6, 6 and 6, and 12 and 6 for 682 and 830 nm, respectively.

roughly the same (~7.5 s), a finding which is consistent with previous research of human visual cortex (e.g., Colier et al., 2001; Obrig et al., 2000; Wobst et al., 2001). It should be noted that although HbT appears to decrease in the first 2–3 s after stimulus onset, we do not find that it changes significantly from 0 ($P \gg 0.05$).

In Fig. 4, we focus on the first 7.5 s of the motor hemodynamic response. In order to examine the effect of the differential pathlength factors on the early portion of the hemodynamic response function, hemoglobin concentrations were calculated with several different differential pathlength pairs (3 to 12 in 0.5 increments for the 682 nm laser, and 6 for the 830 nm laser). We plot 3 of these pairs (3 and 6, 6 and 6, and 12 and 6) for the motor data in Fig. 4 and the visual data in Fig. 5. The intermediate DPF values produce curves that are intermediate to those plotted here. As Fig. 4a shows, the amplitude of the dip (i.e., early HbR increase) decrease as the value of the DPF at 682 nm increases. Within the physiologically plausible DPF range of ±20%, we find that the dip is not significant in the motor data but is in the visual data ($P < 0.05$).

Discussion

Qualitative features of the hemodynamic response function

The hemodynamic response functions measured in the motor and visual paradigms exhibit the expected features as observed by previous fMRI (Kwong et al., 1992; Ogawa et al., 1992) and optical studies (Frostig et al., 1990; Malonek and Grinvald, 1996; Obrig et al., 1996a) of brain activation. The response onset is delayed by approximately 2 s. Then, for the motor paradigm the total and oxyhemoglobin signals rapidly increase, consistent with previous observations of a rapid flow/volume response (Obrig et al., 1996a), while the decrease in deoxyhemoglobin is delayed until approximately 4 s. The HbR response delayed relative to HbT is consistent with washout of HbR from the venous compartment delayed by the vascular transit time (Buxton et al., 1998; Mandeville et al., 1999).

The poststimulus overshoot of HbR has been observed during motor-sensory stimulation since the first fMRI ex-

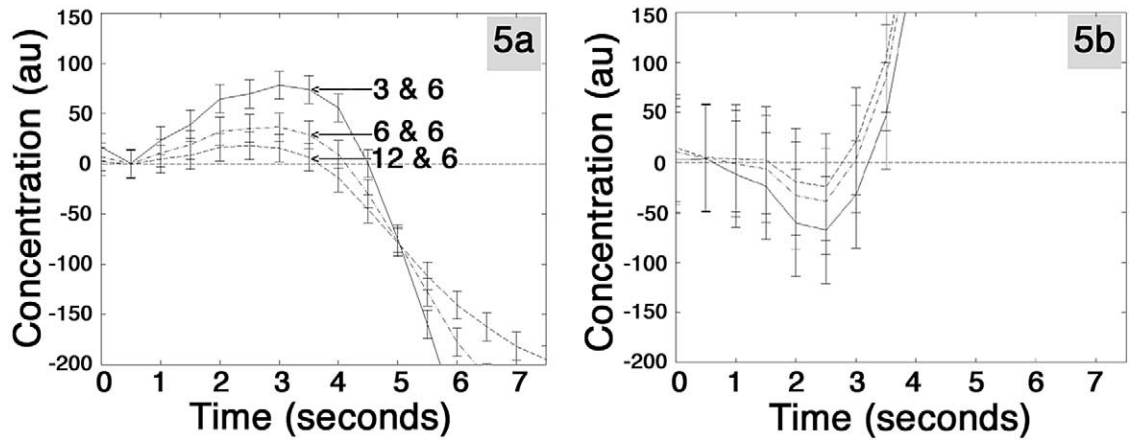

Fig. 5. Initial (a) HbR and (b) HbO_2 response to the visual task analyzed with 3 different differential pathlength factor pairs: 3 and 6, 6 and 6, and 12 and 6 for 682 and 830 nm, respectively.

periments (Kwong et al., 1992). The explanation for this overshoot is:

1. an increase in oxygen extraction fraction (OEF) caused by temporal mismatch between cerebral blood flow (CBF) and cerebral metabolic rate of oxygen ($CMRO_2$) (i.e., CBF returns to baseline before $CMRO_2$) (Frahm et al., 1997; Kruger et al., 1996; Frahm et al., 1996; Ances et al., 2001).
2. an increase in OEF caused by a decrease in blood flow below the baseline value, e.g., a neuronal undershoot with or without coupling of CMRO2 and CBF, and/or
3. a delayed recovery in cerebral blood volume (Mandeville et al., 1998; 1999).

Mandeville's data in rats (Mandeville et al., 1998) and monkeys (Leite et al., 2002) of changes in CBV during brain activation indicate that the HbR overshoot is consistent with their observation of a slow recovery of CBV. However, our data do not show a delayed recovery of HbT, but instead a recovery that is more rapid and undershoots the baseline. The standing assumption is that changes in HbT are proportional to changes in CBV. This is valid provided the local hematocrit level is constant during the activation. The discrepancy between our HbT data and Mandeville's CBV data could result from a decrease in hematocrit following the peak of the HRF. A local decrease in hematocrit could cause an OEF increase which could then lead to an increased HbR concentration. While a hematocrit change could explain the HbR overshoot, it cannot rule out the first and second explanations above.

Qualitatively, the visual data exhibit the same features, though the later onset time relative to the motor result suggests a longer transit time through the vascular bed for the visual activation. By onset time we are referring to the time for HbR decrease and HbO_2 increase. The longer transit time is consistent with the observation of the early dip in HbR as a longer transit time will enhance the dip amplitude (Buxton et al., 1998; Mandeville et al., 1999). We discuss this early response in more detail below. The visual data also exhibit a poststimulus overshoot in HbR and undershoot in HbT. This HbT undershoot is a novel finding that is robust across the two paradigms. The explanation for the undershoot requires a decrease in hematocrit and/or a poststimulus undershoot in CBF. This issue needs to be examined in more detail in the context of neurovascular modeling.

The accuracy of near-infrared spectroscopy

While NIRS techniques are capable of spectroscopic determination of oxy- and deoxyhemoglobin concentrations, complete and reliable separation of the two signals is difficult, particularly with a continuous-wave instrument. There are two categories of errors one must consider: partial volume errors, and cross-talk errors. A partial volume error in a NIRS measurement, by itself, will result in an underestimate of the amplitude of the hemodynamic response (Okada et al., 1997; Boas et al., 2001). Of greater concern are spectral differences in the partial volume effect that, if not properly treated, can cause cross-talk in the estimated hemoglobin changes (Boas et al., 2001; Uludag et al., 2002). That is, changes in HbO_2 can appear as HbR changes and vice versa. The result is that we cannot make accurate statements about the relative magnitudes and temporal onsets of the HbO_2 and HbR response. While imaging arguably best minimizes this cross-talk error, it is possible to reduce sensitivity to cross-talk by positioning the fiber optics so as to elicit a maximum optical response to activation and by optimizing the choice of wavelengths (Boas et al., 2001; Yamashita et al., 2001; Strangman et al., in press). These precautions were taken in our experiments. In particular, we used wavelengths of 682 and 830 nm to minimize cross-talk as has been suggested by (Sevick et al., 1991; Matcher et al., 1995; Yamashita et al., 2001; Strangman et al., in press) and we only considered the data from the detector with the largest percentage signal change out of the four (Strangman et al., in press).

In any NIRS experiment, it is advisable to explore the uncertainty in the calculated hemoglobin concentration changes to address the possibility of cross talk. The concentration calculation depends on the choice of the wavelength-dependent differential pathlength factor, or better named "partial pathlength factor" in the case of localized changes (Hiraoka et al., 1993; Uludag et al., 2002). Experimentally, estimation of the spectral dependence of this pathlength factor is likely to have an uncertainty of 20% or more primarily due to uncertainty in the position and volume of activation, but also resulting from uncertainty in the tissue structure (scalp, skull, etc.) and optical properties (Duncan et al., 1996; Strangman et al., in press). We thus calculated the concentration changes given a wide range of pathlength factors to determine if any features of the data were significantly altered. No significant differences were observed over a $+/-$ 20% range from the initial pathlength factors of 6 and 6 for 682 n and 830 nm, respectively.

Early deoxygenation in the HRF

The results of this study have further implications for discerning the nature of neurovascular coupling insofar as they contribute to our understanding of early deoxygenation in the hemodynamic response. Early deoxygenation, also referred to as the "fast response" or "initial dip," was first reported by Frostig et al. (1990), who found a brief and small increase in the concentration of HbR at the locus of neural activity before HbR decreased. Its presence would appear to challenge the assumption of a tight coupling between neuronal activity and cerebral blood flow as first proposed by Roy and Sherrington (1890), and raise important issues for neuroimaging techniques that are based on the idea that changes in electrical activity are coupled to changes in microcirculation. For example, it may be possi-

ble to increase the spatial resolution of fMRI by mapping this early increase rather than the later and larger decrease in HbR (Duong et al., 2000; Kim et al., 2000).

An early increase in the relative concentration of HbR in the hemodynamic response in the visual cortex of the cat using optical imaging has been reported by several groups (Frostig et al., 1990; Malonek and Grinvald, 1996; Malonek et al., 1997), and in the visual cortex of awake and anesthetized primates (Shtoyerman et al., 2000), demonstrating that early deoxygenation cannot be explained by either differences in species or state of anesthesia. An early HbR increase appears to be most easily found in the visual cortex, but it has also been found with optical imaging in rat barrel cortex (Jones et al., 2001) and in rat primary sensory cortex (Mayhew et al., 1999; Nemoto et al., 1999). Evidence of early deoxygenation is not confined to the results of optical studies, for it has also been detected with fMRI in human visual cortex (Ernst and Hennig, 1994; Menon et al., 1995; Hu et al., 1997; Yacoub and Hu, 1999), in primate visual cortex (Logothetis et al., 1999), and in cat visual cortex (Kim et al., 2000).

However, the existence of an early HbR increase has been questioned by researchers who find it only inconsistently, or not at all. Lindauer et al. (2001) did not find it in rat primary sensory cortex using three different optical methods. Using fMRI, no early HbR increase was found in rat somatosensory cortex by Mandeville et al. (1999) and Marota et al. (1999) or in human visual cortex (Fransson et al., 1998). Jezzard et al. (1997) failed to detect it in cat visual cortex even though their stimulation paradigm and magnet strength were the same as those used in a study that did find the dip (Duong et al., 2000).

The inconsistent results from the optical studies have recently been addressed by Lindauer et al. (2001). They report that they found a dip in rat primary sensory cortex when using a simple constant pathlength analysis. They argue, as have we (Strangman et al., in press), that using a constant pathlength analysis can lead to errors in determining chromophore concentrations via cross-talk. When the same data were analyzed using a differential pathlength analysis the dip vanished, indicating that the method of analysis can be decisive. The authors point out that previous optical imaging research that detected a dip (e.g., Malonek and Grinvald, 1996; Malonek et al., 1997; Nemoto et al., 1999; Shtoyerman et al., 2000) analyzed their data by performing constant pathlength analysis, and so these results must be viewed cautiously. Interestingly, in our data, varying the pathlength parameters did cause the dip to appear and disappear for the motor results, but the dip persisted for the visual results. We argue that the existence of the dip in our visual data cannot be due to an incorrect choice of differential pathlength factors.

Our study contributes to the controversy surrounding the dip by presenting optical data gathered from rapidly presented stimuli in functioning human motor and visual cortex. Our results, which are based on the differential pathlength analysis, suggest that different parts of the human cortex behave differently with respect to the dip. In the visual cortex the initial dip is clearly present and analyzing the visual data with extreme DPF values does not make it disappear. By contrast, the data from the motor cortex does not show a statistically significant dip except at implausible values for the DPFs. These results are in general agreement with previous research, for those who claim to see a dip have primarily imaged visual cortex of various species, while those not seeing the dip have primarily imaged sensorimotor cortex. Though no direct comparisons can be made with our data and rat somatosensory or cat visual data, we have evidence that shows that different cortex in the same species behaves differently with respect to the dip, a finding that could be further examined in nonhuman species.

There are two primary explanations for the early deoxygenation portion of the hemodynamic response to neuronal activation. Grinvald and others (Malonek and Grinvald, 1996) claim that a change in $CMRO_2$ causes HbR to increase locally before HbR can decrease through HbR washout (i.e., a $CMRO_2$ increase before an increase in blood flow and correspondingly HbT). The balloon model of Buxton et al. (1998) posits that the dip is due to the rapid increase in venous blood volume before HbR washout occurs such that it is independent of any change in $CMRO_2$. An early increase in HbT equal to the increase in HbR would support the balloon model explanation for the dip. On the other hand, an increase in HbR significantly larger than HbT would support the view that there is an uncoupling of $CMRO_2$ and CBF. While the visual results qualitatively support the uncoupling model (i.e., HbT remains at zero while HbR increases), it does not statistically support one model over the other (all $P > 0.6$).

While we are unable to support one explanation over the other, it is interesting to note that in either case, a longer transit time for HbR washout increases the magnitude of the observed early response. To our knowledge no one has reported any comparison of capillary transit time across regions of cortex. Our results would suggest that there is a longer transit time in human visual cortex than in motor cortex. Further research is needed to test this hypothesis, but confirmation of such a claim could have significant implications for neuroimaging methods dependent on the hemodynamic response.

Of additional concern is the potential susceptibility to systemic alterations for differing types of stimuli. In particular, it is known that finger tapping in a block design alters the heart rate and induces a systemic increase in oxygenation and blood volume (Franceschini et al., 2000, in press; Wobst et al., 2001). This effect has not been observed for visual stimuli (M.A. Franceschini, personal communication). These systemic effects could confound the interpretation of any neuroimaging measure of the hemodynamic

response function to neuronal activation as follows: the heart rate acceleration synchronized with finger tapping produces an increase in oxygenation and blood volume that would counter and potentially negate an activation-induced early deoxygenation, thus confounding the interpretation of the hemodynamic response function. However, the data presented here were obtained from an event-related design, not a blocked design, which has not previously been investigated in detail in terms of its susceptibility to systemic changes. In this study, when measuring heart rate directly from the raw NIRS data, we found no changes in heart rate between an initial 30 s of baseline data and any 30 s period of data during the presentation of event-related motor (or visual) stimuli. This suggests that systemic alterations likely played a minimal or negligible role in this experiment.

Summary

We acquired NIRS data from humans during performance of simple motor and visual tasks, using rapid-presentation event-related paradigms. The results from this study show that rapid presentation event-related paradigms, when used with NIRS, can provide robust estimates of the hemodynamic response that are free from artifacts due to low-frequency signal components, unlike data from blocked designs. We have shown that such designs will work for the study of motor and visual cortex. The use of rapid presentation designs opens the door to NIRS investigators to ask different kinds of questions than are possible with blocked designs. By using a rapid-presentation event-related design, NIRS researchers may be able to design studies that involve discrimination tasks so that other parts of the human cortex, such as those associated with language or memory, can be studied.

Our results also reveal significant differences in the hemodynamic response in motor and visual cortices. In both the motor and visual data the onset of the increase in HbO_2 occurs before Hb decreases, and there is a poststimulus undershoot. However, we did not find significant early deoxygenation in the motor data using physiologically plausible values for the differential pathlength factor, but did find significant early deoxygenation in the visual data. This difference is consistent with MRI data and could be attributable to different capillary transit times in these cortices and/or may indicate an uncoupling between CMRO2 and CBF for visual-type stimuli in the occipital cortex.

Further research is needed to explain if this explanation is accurate. Finally, our results show that total blood volume (HbT) recovers from peak response before HbO_2 and undershoots the baseline level, suggesting an undershoot in blood flow perhaps arising from poststimulus neuronal inhibition. This effect will have to be considered in future neurovascular models.

Acknowledgments

Gary Jasdzewski thanks John Thompson and Jill Clark for their assistance with several aspects of the study, Sue Hespos for her optode placement technology, Rajeev Raizada for assistance in stimulus development, Joe Mandeville for his comments on neurovascular modeling, and the Alafi Family Foundation for financial support. Gary Strangman acknowledges support from the NIH (P41-RR14075) and the National Space Biomedical Research Institute through NASA Cooperative Agreement NCC 9-58. David Boas acknowledges support from the NIH through R29-NS38842 and P41-RR14075.

References

Ances, B.M., Buerk, D.G., Greenberg, J.H., Detre, J.A., 2001. Temporal dynamics of the partial pressure of brain tissue oxygen during functional forepaw stimulation in rats. Neurosci. Lett. 306, 106–110.

Beese, U., Langer, H., Lang, W., Dinkel, M., 1998. Comparison of near-infrared spectroscopy and somatosensory evoked potentials for the detection of cerebral ischemia during carotid endarterectomy. Stroke 29, 2032–2037.

Boas, D.A., Franceschini, M.A., Dunn, A.K., Strangman, G., 2002. Non-invasive imaging of cerebral activation with diffuse optical tomography, in: Frostig, R. (Ed.), Optical Imaging of Brain Function, CRC Press, Boca Raton, FL.

Boas, D.A., Gaudette, T., Strangman, G., Cheng, X., Marota, J.J.A., Mandeville, J.B., 2001. The accuracy of near infrared spectroscopy and imaging during focal changes in cerebral hemodynamics. NeuroImage 13, 76–90.

Boynton, G.M., Engel, S.A., Glover, G.H., Heeger, D.J., 1996. Linear systems analysis of functional magnetic resonance imaging in human VI . J. Neurosci. 16, 4207–4221.

Buckner, R.L., Bandettini, P.A., O'Craven, K.M., Savoy, R.L., Petersen, S.E., Raichle, M.E., Rosen, B.R., 1996. Detection of cortical activation during averaged single trials of a cognitive task using functional magnetic resonance imaging [see comments]. Proc. Natl. Acad. Sci. USA 93, 14878–14883.

Burock, M.A., Dale, A.M., 2000. Estimation and detection of event-related fMRI signals with temporally correlated noise: a statistically efficient and unbiased approach. Hum. Brain Mapp. 11, 249–260.

Buxton, R.B., Wong, E.C., Frank, L.R., 1998. Dynamics of blood flow and oxygenation changes during brain activation: the balloon model. Magn. Reson. Med. 39, 855–864.

Chance, B., 1991. Optical method. Annu. Rev. Biophys. Biophys. Chem. 20, 1–28.

Colier, W.N., Quaresima, V., Wenzel, R., van der Sluijs, M.C., Oeseburg, B., Ferrari, M., Villringer, A., 2001. Simultaneous near-infrared spectroscopy monitoring of left and right occipital areas reveals contralateral hemodynamic changes upon hemi-field paradigm. Vision Res. 41, 97–102.

Cope, M., Delpy, D.T., 1988. System for long-term measurement of cerebral blood flow and tissue oxygenation on newborn infants by infra-red transillumination. Med. Biol. Eng. Comput. 26, 289–294.

Dale, A., Buckner, R., 1997. Selective averaging of rapidly presented individual trials using fMRI. Hum. Brain Mapp. 5, 329–340.

Dale, A.M., Greve, D.N., Burock, M.A., 1999. Optical stimulus sequences for event-related fMRI. Proc., 5th International Conference on Functional Mapping of the Human Brain, Dusseldorf, Germany.

Duncan, A., Meek, J.H., Clemence, M., Elwell, C.E., Fallon, P., Tyszczuk, L., Cope, M., Delpy, D.T., 1996. Measurement of cranial optical path

length as a functino of age using phase resolved near infrared spectroscopy. Pediatr. Res. 39, 889–894.

Duncan, A., Meek, J.H., Clemence, M., Elwell, C.E., Tyszczuk, L., Cope, M., Delpy, D.T., 1995. Optical pathlength measurements on adult head, calf and forearm and the head of the newborn infant using phase resolved optical spectroscopy. Phys. Med. Biol. 40, 295–304.

Duong, T.Q., Kim, D.S., Ugurbil, K., Kim, S.G., 2000. Spatiotemporal dynamics of the BOLD fMRI signals: toward mapping submillimeter cortical columns using the early negative response. Magn. Reson. Med. 44, 231–242.

Ernst, T., Hennig, J., 1994. Observation of a fast response in functional MR. Magn. Reson. Med. 32, 146–149.

Fallgatter, A.J., Strik, W.K., 1998. Frontal brain activation during the Wisconsin Card Sorting Test assessed with two-channel near-infrared spectroscopy. Eur. Arch. Psychiatry Clin. Neurosci. 248, 245–249.

Frahm, J., Kruger, G., Merboldt, K.D., Kleinschmidt, A., 1996. Dynamic uncoupling and recoupling of perfusion and oxidative metabolism during focal brain activation in man. Magn. Reson. Med. 35, 143–148.

Frahm, J., Krueger, G., Merboldt, K.D., Kleinschmidt, A., 1997. Dynamic NMR studies of perfusion and oxidative metabolism during focal brain activation. Adv. Exp. Med. Biol. 413, 195–203.

Franceschini, M.A., Toronov, V., Filiaci, M., Gratton, E., Fanini, S., 2000. On-line optical imaging of the human brain with 160-ms temporal resolution. Optics Express. 6, 49–57.

Fransson, P., Kruger, G., Merboldt, K.D., Frahm, J., 1998. Temporal characteristics of oxygenation-sensitive MRI responses to visual activation in humans. Magn. Reson. Med. 39, 912–919.

Frostig, R.D., Lieke, E.E., Tso, D.Y., Grinvald, A., 1990. Cortical functional architecture and local coupling between neuronal activity and the microcirculation revealed by in vivo high-resolution optical imaging of intrinsic signals. Proc. Natl. Acad. Sci. USA 87, 6082–6086.

Gratton, G., Corballis, P.M., 1995. Removing the heart from the brain: compensation for the pulse artifact in the photon migration signal. Psychophysiology 32, 292–299.

Hiraoka, M., Firbank, M., Essenpreis, M., Cope, M., Arridge, S.R., van der Zee, P., Delpy, D.T., 1993. A Monte Carlo investigation of optical pathlength in inhomogeneous tissue and its application to near-infrared spectroscopy. Phys. Med. Biol. 38, 1859–1876.

Hock, C., Villringer, K., Muller-Spahn, F., Wenzel, R., Heekeren, H., Schuh-Hofer, S., Hofmann, M., Minoshima, S., Schwaiger, M., Dirnagl, U., Villringer, A., 1997. Decrease in parietal cerebral hemoglobin oxygenation during performance of a verbal fluency task in patients with Alzheimer's disease monitored by means of near-infrared spectroscopy (NIRS)—correlation with simultaneous rCBF-PET measurements. Brain Res. 755, 293–303.

Homan, R.W., Herman, J., Purdy, P., 1987. Cerebral location of international 10–20 system electrode placement. Electroencephalogr. Clin. Neurophysiol. 66, 376–382.

Hu, X., Le, T.H., Ugurbil, K., 1997. Evaluation of the early response in fMRI in individual subjects using short stimulus duration. Magn. Reson. Med. 37, 877–884.

Jezzard, P., Rauschecker, J.P., Malonek, D., 1997. An in vivo model for functional MRI in cat visual cortex. Magn. Reson. Med. 38, 699–705.

Jones, M., Berwick, J., Johnston, D., Mayhew, J., 2001. Concurrent optical imaging spectroscopy and laser-Doppler flowmetry: the relationship between blood flow, oxygenation, and volume in rodent barrel cortex. Neuroimage 13, 1002–1015.

Kim, D.S., Duong, T.Q., Kim, S.G., 2000. High-resolution mapping of iso-orientation columns by fMRI. Nature Neurosci. 3, 164–169 java/Propub/neuro/nn0200_0164.fulltext java/Propub/neuro/nn0200_0164.abstract..

Kohl, M., Lindauer, U., Royl, G., Kuhl, M., Gold, L., Villringer, A., Dirnagl, U., 2000. Physical model for the spectroscopic analysis of cortical intrinsic optical signals. Phys. Med. Biol. 45, 3749–3764.

Kohl, M., Nolte, C., Heekeren, H.R., Horst, S., Scholz, U., Obrig, H., Villringer, A., 1998. Determination of the wavelength dependence of the differential pathlength factor from near-infrared pulse signals. Phys. Med. Biol. 43, 1771–1782.

Kruger, G., Kleinschmidt, A., Frahm, J., 1996. Dynamic MRI sensitized to cerebral blood oxygenation and flow during sustained activation of human visual cortex. Magn. Reson. Med. 35, 797–800.

Kwong, K.K., Belliveau, J.W., Chesler, D.A., Goldberg, I.E., Weisskoff, R.M., Poncelet, B.P., Kennedy, D.N., Hoppel, B.E., Cohen, M.S., Turner, R., Cheng, H.-M., Brady, T.J., Rosen, B.R., 1992. Dynamic magnetic resonance imaging of human brain activity during primary sensory stimulation. Proc. Natl. Acad. Sci. USA 89, 5675–5679.

Leite, F.P., Tsao, D., Vanduffel, W., Fize, D., Sasaki, Y., Wald, L.L., Dale, A.M., Kwong, K.K., Orban, G.A., Rosen, B.R., Tootell, R.B.H., Mandeville, J.B., 2002. Repeated fMRI using iron oxide contrast agent in awake, behaving macaques at 3 T. NeuroImage, in press.

Lindauer, U., Royl, G., Leithner, C., Kuhl, M., Gold, L., Gethmann, J., Kohl-Bareis, M., Villringer, A., Dirnagl, U., 2001. No evidence for early decrease in blood oxygenation in rat whisker cortex in response to functional activation. Neuroimage 13, 988–1001.

Logothetis, N.K., Guggenberger, H., Peled, S., Pauls, J., 1999. Functional imaging of the monkey brain. Nature Neurosci. 2, 555–562 java/Propub/neuro/nn0699_0555.fulltext java/Propub/neuro/nn0699_0555.abstract..

Malonek, D., Dirnagl, U., Lindauer, U., Yamada, K., Kanno, I., Grinvald, A., 1997. Vascular imprints of neuronal activity: relationships between the dynamics of cortical blood flow, oxygenation, and volume changes following sensory stimulation. Proc. Natl. Acad. Sci. USA 94, 14826–14831.

Malonek, D., Grinvald, A., 1996. Interactions between electrical activity and cortical microcirculation revealed by imaging spectroscopy: implications for functional brain mapping. Science 272, 551–554.

Mandeville, J.B., Marota, J.J., Ayata, C., Zaharchuk, G., Moskowitz, M.A., Rosen, B.R., Weisskoff, R.M., 1999. Evidence of a cerebrovascular postarteriole windkessel with delayed compliance. J. Cereb. Blood Flow Metab. 19, 679–689.

Mandeville, J.B., Marota, J.J.A., Kosofsky, B.E., Keltner, J.R., Weissleder, R., Rosen, B.R., Weisskoff, R.M., 1998. Dynamic functional imaging of relative cerebral blood volume during rat forepaw stimulation. Magn. Reson. Med. 39, 615–624.

Marota, J.J.A., Ayata, C., Moskowitz, M.A., Weisskoff, R.M., Rosen, B.R., Mandeville, J.B., 1999. Investigation of the early response to rat forepaw stimulation. Magn. Reson. Med., in press.

Matcher, S.J., Elwell, C.E., Cooper, C.E., Cope, M., Delpy, D.T., 1995. Performance comparison of several published tissue near-infrared spectroscopy algorithms. Anal. Biochem. 227, 54–68.

Mayhew, J., Zheng, Y., Hou, Y., Vuksanovic, B., Berwick, J., Askew, S., Coffey, P., 1999. Spectroscopic analysis of changes in remitted illumination: the response to increased neural activity in brain. NeuroImage 10, 304–326.

Meek, J.H., Elwell, C.E., Khan, M.J., Romaya, J., Wyatt, J.S., Delpy, D.T., Zeki, S., 1995. Regional changes in cerebral haemodynamics as a result of a visual stimulus measured by near infrared spectroscopy. Proc. Roy. Soc. London B 261, 351–356.

Menon, R.S., Ogawa, S., Hu, X., Strupp, J.S., Andersen, P., Ugurbil, K., 1995. BOLD based functional MRI at 4 Tesla includes a capillary bed contribution: echo-planar imaging mirrors previous optical imaging using intrinsic signals. Magn. Reson. Med. 33, 453–459.

Nemoto, M., Nomura, Y., Sato, C., Tamura, M., Houkin, K., Koyanagi, I., Abe, H., 1999. Analysis of optical signals evoked by peripheral nerve stimulation in rat somatosensory cortex: dynamic changes in hemoglobin concentration and oxygenation. J. Cereb. Blood Flow Metab. 19, 246–259.

Obrig, H., Hirth, C., Junge-Hulsing, J.G., Doge, C., Wolf, T., Dirnagl, U., Villringer, A., 1996a. Cerebral oxygenation changes in response to motor stimulation. J. Appl. Physiol. 81, 1174–1183.

Obrig, H., Wenzel, R., Kohl, M., Horst, S., Wobst, P., Steinbrink, J., Thomas, F., Villringer, A., 2000. Near-infrared spectroscopy: does it function in functional activation studies of the adult brain? Int. J. Psychophysiol. 35, 125–142.

Obrig, H., Wolf, T., Doge, C., Hulsing, J.J., Dirnagl, U., Villringer, A., 1996b. Cerebral oxygenation changes during motor and somatosensory

stimulation in humans, as measured by near-infrared spectroscopy. Adv. Exp. Med. Biol. 388, 219–224.

Ogawa, S., Tank, D., Menon, R., Ellermann, J., Kim, S.-G., Merkel, H., Ugurbil, K., 1992. Intrinsic signal changes accompanying sensory stimulation: functional brain mapping with magnetic resonance imaging. Proc. Natl. Acad. Sci. USA 89, 5951–5955.

Okada, E., Firbank, M., Schweiger, M., Arridge, S.R., Cope, M., Delpy, D.T., 1997. Theoretical and experimental investigation of near-infrared light propagation in a model of the adult head. Appl. Optics. 36, 21–31.

Roy, C.S., Sherrington, C.S., 1890. On the regulation of the blood-supply of the brain. J. Physiol. (London) 11, 85–108.

Sakatani, K., Xie, Y., Lichty, W., Li, S., Zuo, H., 1998. Language-activated cerebral blood oxygenation and hemodynamic changes of the left prefrontal cortex in poststroke aphasic patients: a near-infrared spectroscopy study. Stroke 29, 1299–1304.

Schroeter, M.L., Zysset, S., Kupka, T., Kruggel, F., Yves von Cramon, D., 2002. Near-infrared spectroscopy can detect brain activity during a color-word matching Stroop task in an event-related design. Hum. Brain Mapp. 17, 61–71.

Sevick, E.M., Chance, B., Leigh, J., Nioka, S., Maris, M., 1991. Quantitation of time-and frequency-resolved optical spectra for the determination of tissue oxygenation. Anal. Biochem. 195, 330–351.

Shtoyerman, E., Arieli, A., Slovin, H., Vanzetta, I., Grinvald, A., 2000. Long-term optical imaging and spectroscopy reveal mechanisms underlying the intrinsic signal and stability of cortical maps in V1 of behaving monkeys. J. Neurosci. 20, 8111–8121.

Steinbrink, J., Kohl, M., Obrig, H., Curio, G., Syre, F., Thomas, F., Wabnitz, H., Rinneberg, H., Villringer, A., 2000. Somatosensory evoked fast optical intensity changes detected non-invasively in the adult human head. Neurosci. Lett. 291, 105–108.

Steinmetz, H., Furst, G., Meyer, B.U., 1989. Craniocerebral topography within the international 10–20 system. Electroencephalogr. Clin. Neurophysiol. 72, 499–506.

Strangman, G., Franceschini, M.A., Boas, D.A., Factors affecting the accuracy of near-infrared spectroscopy (NIRS) data analysis for focal changes in hemodynamics, submitted for publication.

Uludag, K., Kohl, M., Steinbrink, J., Obrig, H., Villringer, A., 2002. Cross talk in the Lambert-Beer calculation for near-infrared wavelengths estimated by Monte Carlo simulations. J. Biome. Optics 7, 51–59.

Villringer, A., Chance, B., 1997. Non-invasive optical spectroscopy and imaging of human brain function. Trends Neurosci. 20, 435–442.

Villringer, A., Planck, J., Hock, C., Schleinkofer, L., Dirnagl, U., 1993. Near infrared spectroscopy (NIRS): a new tool to study hemodynamic changes during activation of brain function in human adults. Neurosci. Lett. 154, 101–104.

Watanabe, E., Maki, A., Kawaguchi, F., Takashiro, K., Yamashita, Y., Koizumi, H., Mayanagi, Y., 1998. Non-invasive assessment of language dominance with near-infrared spectroscopic mapping. Neurosci. Lett. 256, 49–52.

Wobst, P., Wenzel, R., Kohl, M., Obrig, H., Villringer, A., 2001. Linear aspects of changes in deoxygenated hemoglobin concentration and cytochrome oxidase oxidation during brain activation. NeuroImage 13, 520–530.

Yacoub, E., Hu, X., 1999. Detection of the early negative response in fMRI at 1.5 Tesla. Magn. Reson. Med. 41, 1088–1092.

Yamashita, Y., Maki, A., Koizumi, H., 2001. Wavelength dependence of the precision of noninvasive optical measurement of oxy-, deoxy-, and total-hemoglobin concentration. Med. Phys. 28, 1108–1114.